A Rising Edge based Detection Algorithm for MIMO Molecular Communication

Yu Huang, *Student Member, IEEE,* Xuan Chen, *Student Member, IEEE,* Miaowen Wen, *Senior Member, IEEE,* Lie-Liang Yang, *Fellow, IEEE,* Chan-Byoung Chae, *Senior Member, IEEE,* and Fei Ji, *Member, IEEE*

***Abstract*—In this letter, we propose a low-complexity detection algorithm for multi-input-multi-output (MIMO) molecular communication (MC). By virtue of a rising edge in received signals, this detection algorithm is capable of recovering the information bits in MIMO-MC systems. From an engineering point of view, this algorithm can significantly eliminate the impact of inter-symbol interference. It has also proven itself useful for dealing with the received signal from the MIMO-MC testbed with sufficiently low bit error rate (BER) or even an error-free performance. Moreover, in terms of BER performance, this algorithm outperforms existing detection algorithms for single-input single-output MC systems.**

***Index Terms*—Bit error rate (BER), low-complexity detection, MIMO, molecular communication, rising edge.**

I. Introduction

MOLECULAR communication (MC), inspired by nature, is envisioned to achieve nano-scale communications among nanomachines [1]. The history of MC research is described in [2], where its future path is also envisioned.

Modulation schemes for MC generally exploit molecules concentration (number), type, spatial distribution, and release time to transmit information [3]. Novel asynchronous modulation schemes were presented in [4], where information is modulated between the release time difference of two consecutive transmitted molecules. Asynchronous receiver for timing channel was proposed in [5], lowering the system complexity. In addition to molecule number and release time, concentration difference was regarded as a new metric for signal detection in the nano-scale single-input single-output based MC (SISO-MC) systems, combating the influence of the ISI [6]. Another detection scheme used the first derivative of the received concentration signals for signal detection in the SISO-MC systems, analytically indicating its ISI-mitigation capability [7]. Moreover, the authors in [8] proposed multi-input-multi-output (MIMO)-based MC (MIMO-MC) system as an essential step towards the higher data rate or more reliable link in MC.

Yet, most of the existing MC literature, including the works cited above, studied theoretical MC models, where researchers typically presume the free-diffusion channel with point transmitters and spherical receivers [9], while it may be different from the MC channel in practice. To this end, some recent works have been proposed to fill the gap between the theory and experiments on MC. Specifically, the authors in [10] derived a more realistic channel model based on numerous experiments from a macro-scale MC testbed. A recent MC benchtop testbed that attained 40 bps with sufficiently low BER was demonstrated in [11], where a chemical vapor emitter and a photoionization detectors served as the transmitter and receiver, respectively. As for practical MC detectors, a low-complexity detection algorithm, namely, increase detection algorithm (IDA), was proposed for practical SISO-MC testbed [12]. In addition, a successful demonstration of MIMO-MC prototype was provided in [13], while the detection schemes were based on the theoretical model. How to design a proper detection algorithm for MIMO-MC testbed remains an open problem. To this end, we propose a detection algorithm for both SISO-MC and MIMO-MC systems with on-off keying (OOK) modulation. Note that the error performance of OOK with/without ISI cancellation was thoroughly studied in [14], where Poisson, Gaussian-approximation, simplified Poisson, and simplified Gaussian approaches are used to derived the exact and approximate bit error rates (BERs).

The contribution of this paper is two-fold: first, we propose a low-complexity detection algorithm for the practical MIMO-MC with error-free performance; second, we enhance the BER performance of the detection algorithms when concentration difference is used as the input parameter.

II. System Model

A. Review of MIMO-MC system

Let us first briefly review the principles of the MIMO-MC system by following [3]. In a MIMO-MC system with N_t transmitters and N_r receivers and operated in the spatial multiplexing mode with OOK, transmit signal vector at the release time t is denoted as

$$\mathbf{q}(t) = \Big[q_1(t), \ldots, q_i(t), \ldots, q_{N_t}(t)\Big]^T, \tag{1}$$

where $q_i(t) \in \{0, Q\}$ denotes the number of molecules emitted by the i-th transmitter. With OOK modulation, when bit "0" is

The algorithm in this work is developed by the winner of data bakeoff (molecular MIMO competition) in proceeding of IEEE Communication Theory Workshop (CTW) 2019, Selfoss, Iceland, available at: https://ctw2019.ieee-ctw.org/authors/.

The work of Y. Huang, X. Chen, M. Wen, and F. Ji was supported in part by the National Natural Science Foundation of China under Grant 61871190, and in part by the Natural Science Foundation of Guangdong Province under Grant 2016A030308006. The work of C.-B. Chae was in part supported by the Basic Science Research Program through the National Research Foundation of Korea funded by the Ministry of Education (NRF- 2017R1A1A1A05001439) *(Corresponding author: Miaowen Wen.)*

Y. Huang, X. Chen, M. Wen and F. Ji are with the School of Electronics and Information Engineering, South China University of Technology, Guangzhou 510641, China (e-mail: ee06yuhuang@mail.scut.edu.cn; eechenxuan@mail.scut.edu.cn; eemwwen@scut.edu.cn; eefeiji@scut.edu.cn).

L.-L. Yang is with the Southampton Wireless Group, School of Electronics and Computer Science, University of Southampton, Southampton SO17 1BJ, U.K. (e-mail: lly@ecs.soton.ac.uk).

C.-B. Chae is with the Yonsei Institute of Convergence Technology, School of Integrated Technology, Yonsei University, South Korea (e-mail: cbchae@yonsei.ac.kr).

This article has been accepted for publication in a future issue of this journal, but has not been fully edited. Content may change prior to final publication. Citation information: DOI 10.1109/LWC.2019.2961360, IEEE Wireless Communications Letters

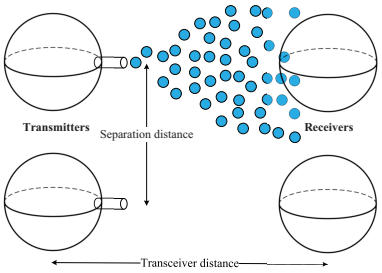

Fig. 1. System diagram of 2×2 MIMO-MC.

transmitted, the i-th transmitter keeps silent, while it releases Q molecules for transmitting bit "1". The channel matrix in MIMO-MC can be expressed as

$$\mathbf{P}(t) = \Big[\mathbf{p}_1(t); \ldots; \mathbf{p}_j(t); \ldots; \mathbf{p}_{N_t}(t)\Big], \tag{2}$$

where the column vector $\mathbf{p}_j(t) \in \mathbb{R}^{N_r \times 1}$ is the channel impulse response (CIR) from the j-th transmitter to all the N_r receivers at time t, given by

$$\mathbf{p}_j(t) = \big[p_{1j}(t), \ldots, p_{ij}(t), \ldots, p_{N_r j}(t)\big]^T, \tag{3}$$

where the entry $p_{ij}(t)$ is the CIR of the i-th receiver in response to the j-th transmitter. Based on (1) and (2), the receiver side can sense the signal vector that goes through the channel at the sampling time t. Given the noise corruption, the received signal vector is given by

$$\begin{aligned}\mathbf{y}(t) &= \Big[y_1(t), \ldots, y_i(t), \ldots, y_{N_r}(t)\Big]^T \\ &= \sum_{l=0}^{L} \mathbf{P}(t + lT_{\text{sym}})\mathbf{q}(t - lT_{\text{sym}}) + \mathbf{n}(t),\end{aligned} \tag{4}$$

where $\mathbf{n}(t)$ is the noise vector, T_{sym} denotes the symbol duration, and L represents the length of ISI. Specifically, $y_i(t)$ is the received signal of the i-th receiver, expressed as

$$y_i(t) = \sum_{j=1}^{N_t} \sum_{l=0}^{L} p_{ij}(t + lT_{\text{sym}}) q_j(t - lT_{\text{sym}}) + n_i(t), \tag{5}$$

where $n_i(t)$ is the noise component of the i-th receiver. When the j-th transmitter and the i-th receiver are assumed to be paired, (5) can be re-written in a more explicit form as

$$y_i(t) = \underbrace{p_{ij}(t) q_j(t)}_{\text{desired signal}} + \underbrace{I_i(t)}_{\text{sum of interference}} + \underbrace{n_i(t)}_{\text{noise}}, \tag{6}$$

where $I_i(t)$ refers to the sum of interference at the i-th receiver that composes ISI and the ILI.

B. Characteristics of CIR

Theoretically, the concentration of the information molecules at the passive receivers can be depicted by Fick's second law of diffusion [14]. When a pulse of Q_j molecules is released by the j-th point transmitter in a 3-D unbounded space, the CIR of the i-th receiver in response to the j-th transmitter at t can be expressed as

$$c_{ij}(t) = \frac{Q_j}{(4\pi D t)^{\frac{3}{2}}} \exp\left(-\frac{{l_{ij}}^2}{4Dt}\right), \tag{7}$$

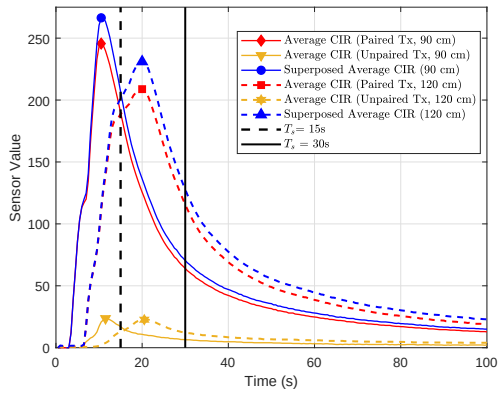

Fig. 2. Average CIRs in an arbitrary receiver of the 2×2 MIMO-MC testbed with various transceiver distances.

where l_{ij} is the distance between the j-th transmitter and the i-th receiver, and D is the diffusion coefficient of information molecules. Despite the theoretical CIR described above, the characteristics of experimental CIR in MIMO-MC are important for the design of an appropriate detection algorithm. To view this, let us follow the experimental 2×2 MIMO-MC system with OOK modulation [13] as shown Fig. 1, where the upper transmitter sends bit "1" by releasing an impulse of information molecules colored in blue, while the lower transmitter keeps silent to send bit "0". In Fig. 1, the text *transceiver distance* indicates the distance between the paired transmitter and receiver, while *separation distance* is the distance between adjacent transmitters or receivers. It is worth noting that, instead of the aforementioned free-diffusion model in (7), this testbed exploits the impulsive force for transmission, the CIR of which was recently studied in [10].

To remove the bias introduced by the experiments and show the CIRs' characteristics accurately, the average CIR is considered based on multiple CIR realizations. In Fig. 2, the average paired and unpaired CIRs, together with their superposition are plotted, respectively, the maximum values of which are highlighted with specific markers. The sampling period T_{sam} for sensor value[1] is 0.5 second, and the separation distance is 30 cm. When the transceiver distance is 90 cm, the maximum sensor values (time) of the paired, unpaired, and superposed CIRs are 245.6 (10.5 s), 23.6 (11.5 s), and 266.4 (10.5 s), respectively, while 208.8 (20 s), 23.6 (20 s), and 266.4 (20.5 s) are obtained for the 120-cm case.

Provided that the transmission energy[2] and separation distance are fixed, Fig. 2 demonstrates that a larger transceiver distance leads to a lower peak sensor value. Besides, the time position of the maximum sensor value is further delayed when the transceiver distance increases. One can easily see that the desired CIR has a more apparent rising trend, referred to as the *rising edge* than that from the unpaired transmitter. Moreover,

[1]The MIMO-MC testbed implements MQ-3 sensor at the receivers to obtain sensor value, which is linearly convertible to a sensor voltage by multiplying 5/1023.

[2]Transmission energy refers to the number of molecules in each release. For a source with uniformly distributed information molecules, a fixed pulse release time can roughly guarantee fixed transmission molecular energy.

This article has been accepted for publication in a future issue of this journal, but has not been fully edited. Content may change prior to final publication. Citation information: DOI 10.1109/LWC.2019.2961360, IEEE Wireless Communications Letters

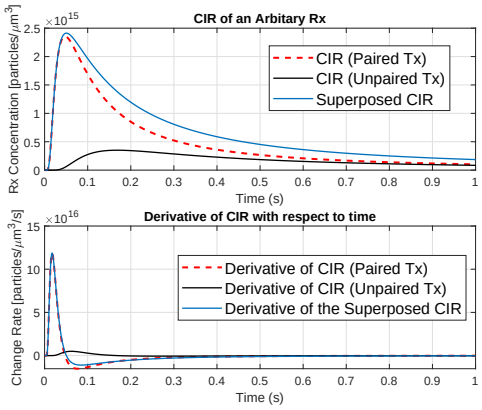

Fig. 3. CIRs and their first derivatives of an arbitrary receiver in a 2×2 MIMO-MC when $Q = 500$, $D = 2.2 \times 10^{-9} m^2/s$, the distance between the desired link is $25\mu m$, and the separation distance between the Txs/Rxs is $40\mu m$.

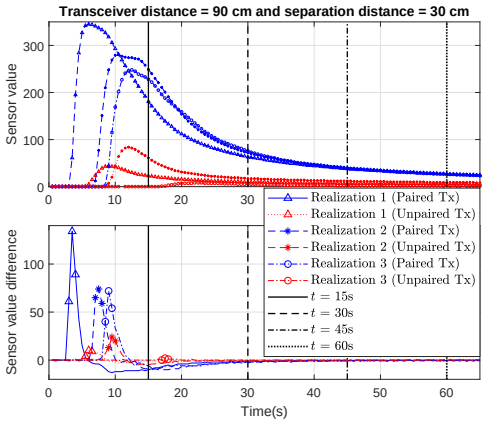

Fig. 4. Desired and undesired CIRs with respect to sensor value in the 2×2 MIMO-MC testbed with transceiver distance being 90 cm.

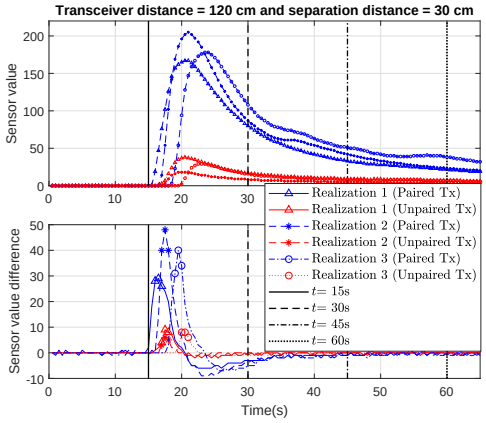

Fig. 5. Desired and undesired CIRs with respect to sensor value in the 2×2 MIMO-MC testbed with transceiver distance being 120 cm.

the superposed CIR, defined as the sum of them, has a similar shape to the desired CIR. However, the CIR then experiences a slow descending phase monotonically, lingering long before vanishing, which causes ISI.

III. Rising Edge Based Detection (RED)

A. Concentration difference as a new metric

Researchers have recently regarded concentration difference as a new metric for the signal detection that allows to achieve, theoretically and experimentally, satisfactory BER performance for SISO-MC [6], [7], [12]. Note that the derivative of the concentration signals of (7) with respect to time can be considered as a specific form of concentration difference [7], which can be expressed as

$$\frac{\partial c_{ij}(t)}{\partial t} = Q_j \left(\frac{{l_{ij}}^2}{32\pi^{\frac{3}{2}} D^{\frac{5}{2}} t^{\frac{7}{2}}} - \frac{3}{16(\pi D)^{\frac{3}{2}} t^{\frac{5}{2}}} \right) \exp\left(-\frac{{l_{ij}}^2}{4Dt} \right). \tag{8}$$

Plotted in Fig. 3 are the theoretical CIRs and their first derivatives with respect to time, given by (7) and (8). Note that the theoretical CIRs in Fig. 3 share a similar trend with their experimental CIRs counterparts shown in Fig. 2, both having a typical rising edge at the beginning of reception. Theoretically, a rising edge, located within the time interval around T_{dp} (the time of first derivative's maximum value), indicates a rapid increase of concentration. Explicitly, the tail of the CIR's first derivative approaches zero more rapidly, suggesting that the effect of the previous symbols can be removed when concentration difference (derivative) is served as a new observation for signal detection. Note that T_{dp} is also shorter than the time interval of the peak concentration value T_{cp}, given by the relationship of $T_{\text{dp}} \approx 0.368 T_{\text{cp}}$ [7].

Inspired by the properties demonstrated in Fig. 3, let us turn to the 2×2 MIMO-MC testbed. For ease of comparison, we plot the realizations of the CIRs (sensor value) obtained by sensors in the upper parts of Figs. 4 and 5. Correspondingly, the sensor value at a given sampling time minus its previously sensed one leads to the sensor value difference, which is demonstrated in the lower parts of Figs. 4 and 5.

Firstly, we observe that the rising edge can be easily detected when several relatively large sensor value differences are obtained consecutively. For ease of observation, these points are highlighted with specific markers in the lower parts of Figs. 4 and 5, respectively. Secondly, the time yielding the maximum sensor value difference is prior to its counterpart sensor value. Thirdly, the desired CIR and ILI can be easily distinguished according to the strength of the sensor values' difference.

From the above analysis and observation, we can conceive that the strength of rising edge can be exploited for information detection in the MIMO-MC testbed.

B. Discrete form of sampled signals

Nowadays, practical systems process discrete signals. For this purpose, the continuous function in (6) can be transformed into the discrete form if the i-th receiver samples the sensor's output every T_{sam} seconds. When at t the n-th sample is obtained, i.e., $n = \frac{t}{T_{\text{sam}}}$. Let the corresponding sensor value at the i-th receiver be expressed as $y_{i,n}$. Then the sequence vector at the i-th receiver is represented by

$$\mathbf{y}_i = [y_{i,1}, \cdots, y_{i,n}, \cdots, y_{i,N}], \tag{9}$$

This article has been accepted for publication in a future issue of this journal, but has not been fully edited. Content may change prior to final publication. Citation information: DOI 10.1109/LWC.2019.2961360, IEEE Wireless Communications Letters

where N is the total number of samples. Correspondingly, a sequence of the sensor value differences can be obtained by the i-th receiver using the *forward difference* operation in (9) as

$$\begin{aligned}\mathbf{d}_i &= \Delta\mathbf{y}_i \\ &= [y_{i,2}-y_{i,1}, \cdots, y_{i,n+1}-y_{i,n}, \cdots, y_{i,N}-y_{i,N-1}] \\ &= [d_{i,1}, \cdots, d_{i,n}, \cdots, d_{i,N-1}], \end{aligned} \tag{10}$$

where Δ is the *forward difference* operator, $d_{i,n}=y_{i,n+1}-y_{i,n}$ is the n-th entry of sequence $\mathbf{d}_i$. It can be shown that for detection of a symbol, only several sensor values are required due to the fact that the rising edge lasts for a relatively short time compared with the proper symbol duration. Specifically, for decoding the b-th symbol at the i-th receiver, where $b = \lceil \frac{t}{T_{\text{sym}}} \rceil$ and $\lceil \cdot \rceil$ refers to the *ceil* operation, $\mathbf{y}_{i,b}$ and its *forward difference* operation $\mathbf{d}_{i,b}$ are taken into account, whose definitions are elaborated in Algorithm 1.

Algorithm 1 RED for MIMO-MC

Input: Received signal $\mathbf{y}_1, \cdots, \mathbf{y}_{N_r}$

Initialization: Thresholds γ_1 and γ_2.

if $\bar{T}_{\text{dp}} < T_{\text{sym}}$ **then**
  $N_e = 0$;
else if $T_{\text{sym}} \leqslant \bar{T}_{\text{dp}} < 2T_{\text{sym}}$ **then**
  $N_e = \frac{\bar{T}_{\text{dp}} - T_{\text{sym}}}{T_{\text{sam}}} + 3$;
else
  Unavailable situation.
end if
for $i = 1 \to N_r$ **do**
  for $b = 1 \to B$ **do**
    $\mathbf{y}_{i,b} = [y_{i,(b-1)N_s+1}, \cdots, y_{i,bN_s+N_e}]$;
    if $N_e > 0$ **then**
      if $b > 1$ **then**
        $\mathbf{d}_{i,b}[1:N_e] = [0, \ldots, 0]$;
      end if
    end if
    $\mathbf{d}_{i,b} = \Delta\mathbf{y}_{i,b} = [d_{i,(b-1)N_s+1}, \cdots, d_{i,bN_s+N_e-1}]$, whose maximum is $d_{i,b,m}$ with position being $m_{i,b}-1$. Update $\mathbf{d}_{i,b} = [0, \mathbf{d}_{i,b}, 0]$ by zero-padding;
    if $d_{i,b,m} \geqslant \gamma_1$ and $\left(\mathbf{d}_{i,b}(m_{i,b}-1) \geqslant \gamma_2$ or $\mathbf{d}_{i,b}(m_{i,b}+1) \geqslant \gamma_2\right)$ **then**
      $\hat{x}_{i,b} = 1$;
    else
      $\hat{x}_{i,b} = 0$;
    end if
  end for
  $\hat{\mathbf{x}}_i = [\hat{x}_{i,1}, \cdots, \hat{x}_{i,B}]$;
end for

Output: Estimated bit sequences are $\hat{\mathbf{x}}_1, \cdots, \hat{\mathbf{x}}_{N_r}$.

C. Description of the detection algorithm

The rationale underlying this algorithm is to detect the existence of a qualified rising edge during several sampling times. In a nutshell, when bit "1" is transmitted by a transmitter, its paired receiver obtains several large positive numbers in vector $\mathbf{d}_{i,b}$, regardless of the bit from the unpaired transmitter, provided that the separation distance is properly set. By contrast, for a transmitted bit "0", the components in $\mathbf{d}_{i,b}$ are either negative, as the result that the adjacent sampling sensor values share similar effects of ISI in MC systems, or small positive values with a weak rising edge generated by ILI. Hence, the rising edge metric provides the ISI-mitigation capability without extra calculation, meaning that the ISI from the paired and unpaired transmitters can be effectively combated.

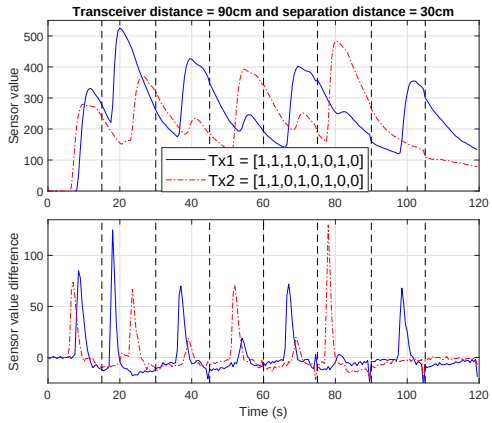

Fig. 6. Sensor value and its difference at receivers with specific bit sequences with transceiver distance being 90 cm.

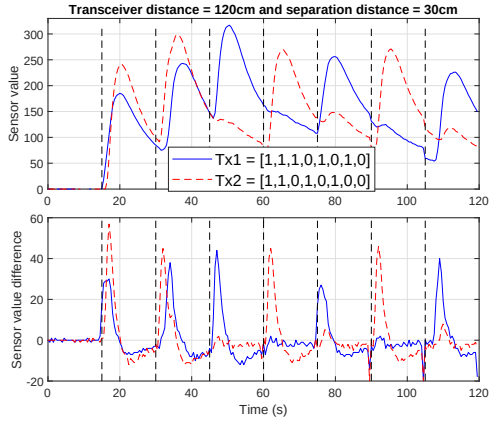

Fig. 7. Sensor value and its difference at receivers with specific bit sequences with transceiver distance being 120 cm.

As described above, one may note that ILI may generate a relatively weak rising edge in the case when the paired transmitter sends bit "0", while the unpaired one transmits bit "1", known as a false-alarm scenario. In this case, the IDA method [12] that counting the number of positive sensor value differences is no longer available for the MIMO-MC case. In order to circumvent this problem, the strength of a rising edge compared with appropriate thresholds is considered in our RED algorithm, the pseudo-code in Algorithm 1. The details on parameters are illustrated below: N_r is the number of pairs in MIMO-MC; B is the length of bits sent by each transmitter; $\bar{T}_{\text{dp}}$ is the mean sampling time with the maximum sensor value difference based on multiple CIR realizations; γ_1 and γ_2 are the distance-dependent thresholds for determining

This article has been accepted for publication in a future issue of this journal, but has not been fully edited. Content may change prior to final publication. Citation information: DOI 10.1109/LWC.2019.2961360, IEEE Wireless Communications Letters

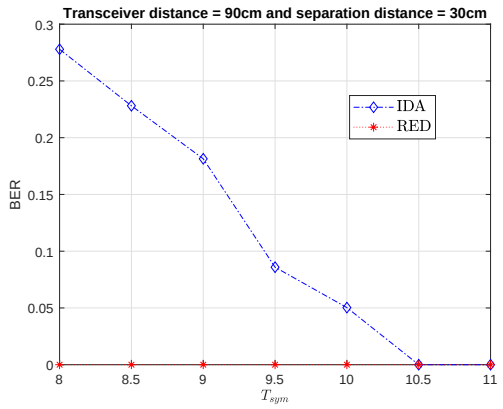

Fig. 8. Comparison of the BER performance between the RED algorithm and IDA.

the rising edge according to the input CIRs; the number of sampling sensor values during each symbol duration is $N_s = \frac{T_{\text{sym}}}{T_{\text{sam}}}$ and N_e is the extended length value, depending on the symbol duration T_{sym}. The introduction of N_e is based on the consecutive symbol transmission, as shown in Figs. 6 and 7 concerning the sensor values and their differences. When the transceiver distance is 90 cm, $\bar{T}_{dp}$ is less than $T_{\text{sym}} = 15$ s, hence, $N_e = 0$, meaning that no extended sampling sensor values are required. When the transceiver distance is 120 cm, however, $\bar{T}_{dp}$ is between $T_{\text{sym}} = 15$ s and $T_{\text{sym}} = 30$ s. In this case, extended sampling sensor values should be considered. This is because that the rising edge of a previous symbol can affect the detection of the current symbol under this setting. Specifically, a invalid rising edge can be presented at the beginning of the symbol, when bit "1" was transmitted previously. To avoid this problem, we can set several front sampling sensor values to zero.

D. Numerical results

Our RED algorithm shows a satisfactory performance in dealing with the test data, which is the sampled sensor values of two receivers from the testbed in [13]. Various parameter settings are provided below: the symbol duration $T_{\text{sym}} = [15, 30]$ s; the paired transceiver distances are selected as 90 cm, 100 cm, 110 cm and 120 cm, resulting in 8 cases in total. Each case has 10 realizations, and each transmitter has 10,000 symbols per realization. With the aim of minimizing the error performance, appropriate threshold selection can be implemented via brute-force search in a specific interval. Hence, a relatively low BER, i.e., 4×10^{-5}, can be achieved in the case that the paired transceiver distance is 120 cm and $T_{\text{sym}} = 15$ s, while all the other cases display error-free performance. In addition, this algorithm can be applicable to the SISO-MC system by setting $N_r = 1$. In Fig. 8, our RED algorithm shows error-free performance in the given interval of symbol duration with $\gamma_1 = 20$ and $\gamma_2 = 15$, while the BER of IDA shows a descending trend with the increasing symbol duration. The IDA attains the same performance as the RED when T_{sym} is greater than 10.5 s. For a fair comparison, IDA uses the optimal parameters via brute-force search that leads to the best BER performance.

IV. Conclusions

In this letter, we proposed a RED algorithm for the macro-scale MIMO-MC testbed. The sensor value difference was considered as the new metric for signal detection, showing the ISI-mitigation capability. With the proper threshold selection, the RED algorithm can attain excellent BER performance. When applied to SISO-MC systems, the RED algorithm is capable of significantly outperforming the IDA algorithms.

Acknowledgment

Yu Huang, Xuan Chen and Miaowen Wen would like to thank Prof. Urbashi Mitra and Prof. Erik G. Larsson for their organization of the first data bakeoff competition at IEEE CTW 2019, and Mr. Changmin Lee, who provided the data from the MIMO-MC prototype that significantly helped the development of the algorithm in this letter. They also highly recognize the contributions made by other participants in this competition.

References

[1] N. Farsad *et al.*, "A comprehensive survey of recent advancements in molecular communication," *IEEE Commun. Survey & Tut.*, vol. 18, no. 3, pp. 1887–1919, third quarter 2016.

[2] T. Nakano, "Molecular communication: A 10 year retrospective," *IEEE Trans. Mol. Biol. Multi-Scale Commun.*, vol. 3, no. 2, pp. 71–78, June 2017.

[3] Y. Huang, M. Wen, L.-L. Yang, C. Chae, and F. Ji, "Spatial modulation for molecular communication," *IEEE Trans. Nanobiosci.*, vol. 18, no. 3, pp. 381–395, July 2019.

[4] N. Farsad, Y. Murin, W. Guo, C. Chae, A. W. Eckford, and A. Goldsmith, "Communication system design and analysis for asynchronous molecular timing channels," *IEEE Trans. Mol. Biol. Multi-Scale Commun.*, vol. 3, no. 4, pp. 239–253, Dec. 2017.

[5] Q. Li, "The clock-free asynchronous receiver design for molecular timing channels in diffusion-based molecular communications," *IEEE Trans. Nanobiosci.*, vol. 18, no. 4, pp. 585–596, Oct. 2019.

[6] B. Li, M. Sun, S. Wang, W. Guo, and C. Zhao, "Low-complexity noncoherent signal detection for nanoscale molecular communications," *IEEE Trans. Nanobiosci.*, vol. 15, no. 1, pp. 3–10, Jan. 2016.

[7] H. Yan, G. Chang, Z. Ma, and L. Lin, "Derivative-based signal detection for high data rate molecular communication system," *IEEE Commun. Lett.*, vol. 22, no. 9, pp. 1782–1785, Sept. 2018.

[8] L. S. Meng, P. C. Yeh, K. C. Chen, and I. F. Akyildiz, "MIMO communications based on molecular diffusion," in *Proc. IEEE Global Commun. Conf. (GLOBECOM)*, Anaheim, CA, USA, Dec. 2012, pp. 5380–5385.

[9] Y. Huang, M. Wen, C. Lee, C. Chae, and F. Ji, "A two-way molecular communication assisted by an impulsive force," *IEEE Trans. Ind. Informat.*, vol. 15, no. 5, pp. 3048–3057, May 2019.

[10] N. Kim, N. Farsad, C. Lee, A. W. Eckford, and C. Chae, "An experimentally validated channel model for molecular communication systems," *IEEE Access*, vol. 7, pp. 81 849–81 858, 2019.

[11] M. Ozmen, E. Kennedy, J. Rose, P. Shakya, J. K. Rosenstein, and C. Rose, "High speed chemical vapor communication using photoionization detectors in turbulent flow," *IEEE Trans. Mol. Biol. Multi-Scale Commun.*, vol. 4, no. 3, pp. 160–170, Sept. 2018.

[12] H. Zhai, Q. Liu, A. V. Vasilakos, and K. Yang, "Anti-isi demodulation scheme and its experiment-based evaluation for diffusion-based molecular communication," *IEEE Trans. Nanobiosci.*, vol. 17, no. 2, pp. 126–133, Apr. 2018.

[13] B. Koo, C. Lee, H. B. Yilmaz, N. Farsad, A. Eckford, and C. Chae, "Molecular MIMO: From theory to prototype," *IEEE J. Sel. Areas Commun.*, vol. 34, no. 3, pp. 600–614, Mar. 2016.

[14] L. Shi and L.-L. Yang, "Error performance analysis of diffusive molecular communication systems with On-Off Keying modulation," *IEEE Trans. Mol. Biol. Multi-Scale Commun.*, vol. 3, no. 4, pp. 224–238, Dec. 2017.